

DNA methylation-dependent chromatin fiber compaction in vivo and in vitro: requirement for linker histone

MIKHAIL A. KARYMOV,^{*,1,2} MIROSLAV TOMSCHIK,^{*,1,3}
SANFORD H. LEUBA,^{*,4} PAOLA CAIAFA,[†] AND JORDANKA ZLATANOVA^{‡,4}

*Physical Molecular Biology, Laboratory of Receptor Biology and Gene Expression, National Cancer Institute, National Institutes of Health, Bethesda, Maryland 20892-5055, USA; [†]Department of Cellular Biotechnology and Haematology, University of Rome 'La Sapienza', 00161 Rome, Italy; and [‡]Department of Chemistry and Chemical Engineering, Polytechnic University, Brooklyn, New York 11201, USA

ABSTRACT Dynamic alterations in chromatin structure mediated by postsynthetic histone modifications and DNA methylation constitute a major regulatory mechanism in DNA functioning. DNA methylation has been implicated in transcriptional silencing, in part by inducing chromatin condensation. To understand the methylation-dependent chromatin structure, we performed atomic force microscope (AFM) studies of fibers isolated from cultured cells containing normal or elevated levels of m⁵C. Chromatin fibers were reconstituted on control or methylated DNA templates in the presence or absence of linker histone. Visual inspection of AFM images, combined with quantitative analysis of fiber structural parameters, suggested that DNA methylation induced fiber compaction only in the presence of linker histones. This conclusion was further substantiated by biochemical results.—Karymov, M. A., Tomschik, M., Leuba, S. H., Caiafa, P., Zlatanova, J. DNA methylation-dependent chromatin fiber compaction in vivo and in vitro: requirement for linker histone. *FASEB J.* 15, 2631–2641 (2001)

Key Words: histone H1 • chromatin fibers • atomic force microscopy

IT IS WIDELY accepted that cytosine methylation in CpG dinucleotides presents an important mechanism of gene regulation (1). It is clear now that at least four different types of genes are controlled by DNA methylation (or the absence thereof) through a series of complex changes in their methylation pattern during development and differentiation: housekeeping genes, tissue-specific genes, imprinted genes, and X-chromosome-linked genes (recently reviewed in refs 2–5). It is also becoming increasingly evident that DNA methylation is intimately linked to cancer and other diseases (for reviews, see refs 6, 7). The discovery during the past decade of proteins that preferentially bind to methylated DNA (8–10) has turned attention to their possible participation in gene silencing, often through recruitment to specific methylated gene regions of histone deacetylases (for reviews, see refs 5, 11, 12).

The involvement of chromatin structure in the DNA methylation-mediated regulation of transcription was demonstrated convincingly in the late 1980s by following the transcription activity of genes microinjected in cultured cells (13). Similar experiments were later performed in *Xenopus* oocytes (14). Ingenious experiments using transformation with patch-methylated plasmid constructs have suggested that decreased accessibility of chromatin DNA to restriction endonucleases (interpreted as chromatin compaction) spreads from focal points of methylation (15). The realization that chromatin structure may be involved in the effect of DNA methylation on transcription has led to studies on possible structural changes in chromatin caused by DNA methylation. Somewhat increased affinity of methylated DNA for histone octamers has been reported (16, 17), but no significant changes in the fine structure of the core particle have been detected (18). Nucleosome placement or positioning was unaffected by DNA methylation in some sequences (17–19), whereas other sequences seemed to exclude nucleosomes when methylated (20). Earlier work reported the disappearance of nucleosome-free regions in gene promoters on methylation (21). Various studies agree that the level of m⁵C is higher in core than in linker DNA (ref 22 and references cited therein). More research is needed to understand chromatin structure changes brought about by DNA methylation.

To elucidate the effect of DNA methylation on chromatin structure, we used chromatin fibers isolated from control NIH/3T3 mouse fibroblasts and from fibroblasts that had been treated with 3-aminobenz-

¹ These authors contributed equally to this work.

² On leave from the Research Institute of Physics, St. Petersburg State University, 198904 St. Petersburg, Russia.

³ On leave from the Institute of Biophysics, Academy of Sciences of the Czech Republic, 612 65 Brno, Czech Republic.

⁴ Correspondence: Department of Chemistry and Chemical Engineering, Polytechnic University, Six MetroTech Center, Brooklyn, NY 11201, USA. E-mail: jzlatano@duke.poly.edu; leuba@nih.gov

amide (3-ABA), a drug that introduces new methyl groups into the 5' position of cytosine residues in CpG dinucleotides (23–26). AFM imaging and quantitative measurements of center-to-center internucleosomal distances, angles formed by consecutive linkers, and number of nucleosomes per unit fiber length showed that DNA hypermethylation causes chromatin fibers to compact.

To better understand the contribution of the different histone classes (core vs. linker) to the observed methylation-dependent chromatin compaction and to see whether the *in vivo* compaction requires methyl-CpG binding proteins, additional experiments were conducted on *in vitro* reconstituted chromatin fibers. The AFM results on these fibers were backed by analysis of micrococcal nuclease (MNase) digestion patterns and sucrose density gradient centrifugation. The data demonstrate unequivocally a requirement for linker histone (LH) binding in order for DNA methylation-dependent compaction to occur. The *in vitro* results also rule out drug-induced changes in poly(ADP-ribosylation) as a cause for the compaction seen *in vivo*.

MATERIALS AND METHODS

Cell culture and preparation and characterization of chromatin fibers

NIH/3T3 cells were grown in Dulbecco modified Eagles minimal essential medium with 10% fetal calf serum and treated with 2 mM 3-ABA for 24 h (23, 24, 26).

Soluble chromatin fibers were prepared as described (27) and characterized by MNase digestion (28). The protein content of the fibers was assessed by SDS-polyacrylamide gel electrophoresis (SDS-PAGE) (29).

Purification of DNA and histones

208–12 DNA was prepared by digestion of plasmid pPol1208 (30) with *Hinc*I and subsequent gel filtration on Sephacryl S500-HR using an FPLC system (Pharmacia, Piscataway, NJ). Chicken histone octamers and H1 were purified from frozen packed chicken erythrocytes (Pel Freeze) using hydroxyapatite and CM-Sephadex chromatography, respectively (31, 32).

DNA methylation

208–12 DNA was methylated using *Sss*I methylase (New England Biolabs, Beverly, MA) and subsequently purified by phenol-chloroform extraction and ethanol precipitation. The degree of methylation was checked by digestion with *Hpa*II and *Msp*I (New England Biolabs), both at 10 U/ μ g of DNA for 2 h. Only DNA fully protected from *Hpa*II digestion was used for further experiments.

Chromatin reconstitution and characterization

Reconstitution was performed by salt dialysis (33); 10 μ g of 208–12 DNA (control or methylated) was mixed with 10 μ g of purified chicken octamers in 2 M NaCl, 10 mM Tris-HCl (pH 7.5), 0.5 mM EDTA and subsequently dialyzed at 4°C against 1 M, 0.75 M, 0.5 M (when LHs were also reconstituted) and 10 or 0 mM NaCl, each containing 10 mM Tris-HCl (pH 7.5), 0.5

mM EDTA, using Slide-A-Lyser (Pierce, Rockford, IL). Each dialysis step was carried out for at least 3 h, the last one usually for 9 h.

To reconstitute chromatin fibers containing LH, histone H1 was added at the 0.5 M NaCl dialysis step and the sample was further dialyzed against 0.5 M NaCl and the low-salt buffer. The presence of bound LHs was verified by purification of the reconstituted fibers by Centricon centrifugation, analyzing the protein content by SDS-PAGE, and MNase verification of the chromatinosome pause (Fig. 3E).

The quality of reconstitution was checked by methidium-propyl-EDTA-iron(II) (MPE) hydrolysis (34–36). The reaction was performed for 10 min in 10 μ l, using freshly prepared 3 μ M MPE complex and stopped by adding 4 \times SDS loading buffer containing 20 mM bathophenanthroline disulfonic acid (Sigma, St. Louis, MO). Samples were electrophoresed on a 1.6% agarose gel in 1 \times TAE. Gels were stained with SYBR Gold (Molecular Probes, Eugene, OR) and washed in water before scanning on Storm 860 (Molecular Dynamics, Sunnyvale, CA).

For MNase digestions, EDTA was omitted from the dialysis buffers and Tris-HCl was replaced by TEA (triethanolamine-HCl, pH 7.5) to facilitate subsequent glutaraldehyde fixation needed for the AFM imaging. One to five units of MNase (Worthington, Freehold, NJ) were added to 8–9 μ l of chromatin sample and incubated at 37°C for 2–30 min. The reaction was stopped by adding 4 \times SDS loading buffer containing 50 mM EDTA. Agarose gel electrophoresis and subsequent analysis were as for MPE. Before analyzing the samples on 6% PAGE (in 1 \times TBE), samples were treated with proteinase K, phenol/chloroform extracted and ethanol precipitated.

Sucrose density gradient centrifugation

Unmethylated 208–12 DNA was end-labeled by Cy5-dCTP (Pharmacia) using Klenow fragment (New England Biolabs). Cy5-labeled control and unlabeled methylated chromatin fibers were mixed and applied onto the top of a 15–30% sucrose gradient in 10 mM TEA-HCl (pH 7.6). The gradient was prepared in 11 ml ultracentrifugation tubes by self-diffusion of equal volumes of 15% and 30% sucrose solutions in the cold (<http://133.71.125.239/english/methods/gradient.htm>). The sample was centrifuged at 36,000 rpm in SW41 Ti rotor for 11 h at 4°C and fractions were collected from the bottom of the tube. Ten microliters of each fraction was made 0.3% in SDS, proteinase K was added to a final concentration of 100 μ g/ml, and the samples were incubated at 37°C for 2 h. Analysis was by 1.2% agarose gel electrophoresis run in 1 \times TAE for 90 min at 80 V. A blue fluorescence scan of total DNA (SYBR Gold staining) and a red fluorescence scan (Cy5 fluorescence) were obtained sequentially on Storm 860.

AFM imaging and analysis

Chromatin fibers ($A_{260}=2$) in 10 mM TEA-HCl, pH 7.5, 0.1 mM EDTA were fixed with 0.1% glutaraldehyde overnight. Fixation was done to avoid possible effects of shearing forces during attachment to the surface and the subsequent washing step (37). Two microliters of sample was deposited on freshly cleaved mica for 1 min, rinsed with five drops of Milli-Q (Millipore, Bedford, MA) water, and fluxed with argon to remove the visible liquid (38). Imaging was performed on a MacMode AFM (Molecular Imaging), using magnetically coated silicon nitride probes oscillated above the surface at a frequency of \sim 100 kHz. The amplitude of oscillation was kept constant at \sim 5 nm during the scanning by piezo height compensation. Each set of experiments was repeated at least

three times using, whenever possible, the same tip to image both control and treated samples. Using the same tip equalizes the broadening effect of the tip over images to be directly compared.

Center-to-center distances between adjacent nucleosomes and angles formed by the intersection of the two lines connecting the centers of three consecutive nucleosome centers were measured as described (32, 39). Only regions of fibers clearly separated from other fibers were selected for measuring the number of nucleosomes per 10 nm of fiber contour length.

RESULTS

Biochemical characterization and AFM imaging of chromatin fibers with normal or increased levels of *in vivo* cytosine methylation

To understand the structural changes in chromatin fibers brought about by cytosine methylation, we studied (with the help of AFM) chromatin fibers isolated from NIH/3T3 control cells and cells that had been treated with 3-ABA. Such treatment introduces new methyl groups into the 5' position of cytosine residues in CpG dinucleotides (50–60% increase over the untreated controls), thus allowing us to compare fibers with 'normal' levels of methylation vs. fibers containing additional methyl groups. The target of 3-ABA is poly(ADP-ribose) polymerase (40), and the reduced poly(ADP-ribosyl)ation of a specific LH subtype may be responsible for the increased DNA methylation level (41). The 3-ABA-induced DNA hypermethylation causes cytologically detectable increases in both the number and the areas of heterochromatic regions, coincident with an increase in the density labeling of these regions with anti-m⁵C monoclonal antibodies (25).

Chromatin fibers solubilized by MNase treatment of nuclei were obtained from control and 3-ABA-treated NIH/3T3 cells. Prolonged MNase digestion was used to exclude from the analysis the most extended chromatin fibers whose structure is expected to be affected most by drug-induced inhibition of poly(ADP-ribosyl)ation (42). Such prolonged digestion was expected to result in chromatin fractions enriched in methylated cytosines, as reported (reviewed in ref 43). The MNase digestion ladders of the solubilized chromatin fibers were indistinguishable for the control and 3-ABA-treated cells (not shown), indicating no major changes in the nucleosomal repeat length between the two cell populations. The protein patterns (not shown) demonstrated that 3-ABA treatment did not lead to any significant alterations in the histone complement either. Histone H1 was present in equal stoichiometries in both the control and treated cells.

Chromatin fibers were fixed with glutaraldehyde and imaged in air, at ambient humidity, with the MacMode AFM. By necessity, fibers were deposited on the surface from low ionic strength buffer. Imaging of chromatin fibers at moderate salt concentrations (40 mM NaCl

and beyond) does not allow the nucleosome resolution needed to quantify fiber parameters (36, 44). Representative images are shown in **Fig. 1A** (control fibers) and **B** (fibers from 3-ABA-treated cells). Control fibers closely resembled fibers isolated from HeLa cells (44) and exhibited a more extended arrangement of nucleosomes than fibers from 3-ABA-treated cells.

Normalized distributions of center-to-center distances between adjacent nucleosomes in chromatin fibers are presented in **Fig. 2A, B**. The quantitative data agree with the visual inspection of images. The center-

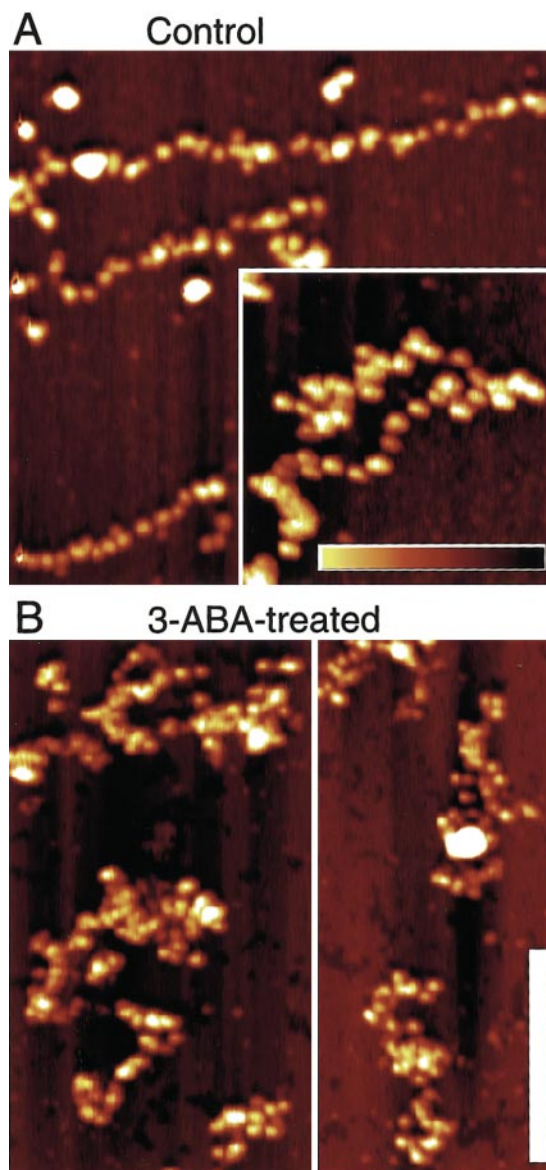


Figure 1. MacMode AFM images of chromatin fibers isolated from NIH/3T3 cells. Chromatin fibers were fixed with 0.1% glutaraldehyde in 10 mM TEA-HCl, pH 7.5, 0.1 mM EDTA and deposited on freshly cleaved mica for imaging in air. Heights from 0 to 5 nm are coded in color, with low areas depicted in dark brown and higher areas depicted in ever increasingly brighter colors as indicated by the horizontal bar. All images are of the same dimensions with the vertical bar being 300 nm. A) Control chromatin fibers. B) Chromatin fibers from 3-ABA-treated cells.

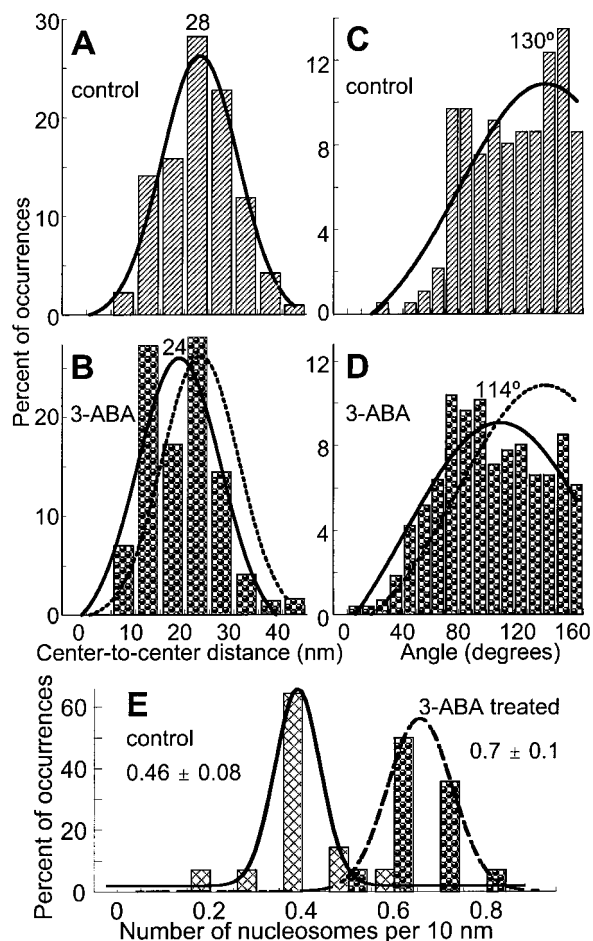


Figure 2. Normalized distributions of distances between centers of adjacent nucleosomes and angles between successive linkers. *A*) Center-to-center distances for fibers from control cells. *B*) Center-to-center distances for fibers from 3-ABA-treated cells. Mean center-to-center distances \pm SE are 28.2 ± 0.4 nm and 24.0 ± 0.2 nm, with 413 and 819 data points in panels *A* and *B*, respectively. Gaussian fits to the distributions are overlaid (*B*) to demonstrate the center-to-center distance shift. *C*, *D*) Distributions of angles between successive linkers in fibers from control and 3-ABA-treated cells, respectively. Note that angle measurements will not discriminate between pairs of angles equally distant from 180° , e.g., an angle of 190° will be recorded as 170° , an angle of 200° will be recorded as 160° , etc. This gives rise to the apparent cutoff at 180° and the corresponding appearance of a 'half' bell curve. Mean angles \pm SE are $130 \pm 3^\circ$ and $114 \pm 2^\circ$, respectively. Gaussian fits are overlaid (*D*) to demonstrate the angle shift. *E*) Frequency distributions of the number of nucleosomes per 10 nm of fiber contour length. Mean numbers \pm SE are 0.46 ± 0.08 and 0.7 ± 0.1 , respectively. Gaussian fits are overlaid to demonstrate the shift in that parameter.

to-center distances for the control fibers centered around 28 nm, as expected on the basis of the known repeat length in cultured cells (45). There was a ~ 4 nm reduction in this parameter for fibers isolated from treated cells. Similar differences between control and experimental samples were observed in two other experiments, although the absolute values differed somewhat from experiment to experiment, possibly as a result of collecting the cells at slightly different growth stages (46).

Figure 2*C*, *D* are histograms of distributions of angles between successive linkers. For control fibers, angles spread from 80° to 180° (Fig. 2*C*). This broad distribution is typical for linker histone containing chromatin, and significantly differs in shape from that of linker histone-depleted fibers (see fig. 4 in ref 44). The half bell-shaped form of this distribution (see legend to Fig. 2) is an indication that no major loss of LHs occurred during isolation (in accordance with the gel analysis) and imaging procedures. Fibers from 3-ABA-treated cells exhibited a noticeable shift of the distribution to lower angles (Fig. 2*D*). Such a shift would indicate fiber compaction, in accordance with earlier predictions (47, 48) and experimental measurements (49).

Finally, we measured the number of nucleosomes per unit contour length of the fiber (Fig. 2*E*). This parameter has been used in earlier physical and electron microscopy studies (45). The mean value for the control fibers was 0.46 ± 0.08 and that for the 3-ABA-treated cells was 0.7 ± 0.1 nucleosomes per 10 nm, pointing to a more compact structure in the latter.

The 208–12 chromatin fiber reconstituted in vitro: biochemical characterization and AFM imaging

Since 3-ABA was first described to affect the activity of poly(ADP-ribose)polymerase (40) and it is well known that poly(ADP-ribosylation) is involved in chromatin organization essentially through modification of LHs (50), it was necessary to discriminate between the direct effect of the drug on poly(ADP-ribosylation) and its indirect effect on DNA methylation. Such discrimination could be achieved by using a system in which the only difference in chromatin fibers would be the extent of cytosine methylation, with otherwise identical histone complement. In the absence of any known in vivo system that would possess such characteristics, we turned to the widely used system for in vitro reconstituted fibers based on the tandemly repeated sequence of the 5S rRNA gene from the sea urchin *Lytechinus variegatus* (51) (Fig. 3*A*, *B*). The overall structure of these fibers is considered to be quite regular, since each 208 bp repeat positions a single nucleosome at one (or several closely situated) position(s) (51–55). Moreover, it contains 12 CpG methylation sites (Fig. 3*B*), eight in the (major) core particle and four in the linker DNA. Thus, when fully methylated on both strands, each 208 bp repeat will contain 24 methyl groups. Such density of methylatable sites is unusually high, greatly exceeding the density in bulk chromatin and similar to that in CpG islands in promoters of housekeeping genes (56). A similar 5S rDNA sequence from the frog *Xenopus borealis* was used in earlier experiments aimed at understanding the effect of DNA methylation on the structure of reconstituted mononucleosomal particles and their affinity for LH binding (17).

Reconstitution of nucleosomal arrays on the 208–12 sequence was performed by salt dialysis. The quality of reconstitution was verified by MPE hydrolysis. MPE is a small chemical endonuclease (34) that preferentially hy-

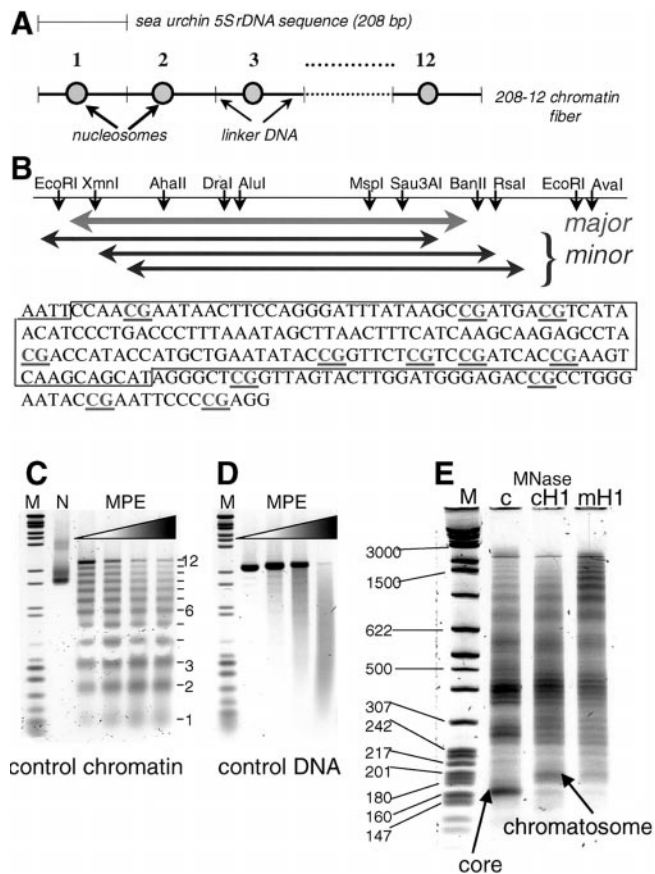


Figure 3. The 208–12 DNA and biochemical characterization of the reconstituted fibers on control and methylated DNA. *A*) Schematic presentation of the 208–12 DNA construct used for reconstitutions. *B*) Restriction map and nucleotide sequence of a single 208 bp repeat. The arrows below the map denote the major and minor nucleosome positions, as determined by Meersseman et al. (54). The major core position is boxed in the sequence and the CpG methylation sites are presented in underlined letters. *C*) DNA products of partial MPE digestion of nucleosomal arrays reconstituted on control unmethylated DNA. The triangle denotes increased concentrations of MPE (1.5–6 μ M). Lane M, size markers; next lane, 208–12 DNA reconstituted with core histones (native lane, N). Numbers on right side of gel indicate the nucleosomal ladder. *D*) Control MPE digestion of naked 208–12 DNA. *E*) DNA products of partial MNase digestion of control nucleosomal arrays (c), chromatin fibers after histone H1 binding to such arrays (cH1), and chromatin fibers after histone H1 binding to methylated arrays (mH1). Lane M, size markers. The core and the chromatosome pauses are denoted on the side. The DNA was run on 6% polyacrylamide gels in TBE buffer. Note also that the methylated H1-containing reconstitute was digested more slowly than the other reconstitutes (see text and Fig. 6A).

drolyses chromatin DNA in the linker regions (35). Indeed, when reconstituted chromatin fibers were partially cleaved with MPE, a nucleosomal ladder that extended < 12 nucleosomes was observed on agarose gels (Fig. 3C). The nucleosome ladder was not affected by performing the reconstitution on the methylated DNA template, or by the presence of histone H1 (not shown).

Additional analysis ensured that histone H1 bound to the nucleosomal arrays correctly, i.e., that reconstitutes

containing H1 showed the chromosome pause in the course of MNase digestions (57). As Fig. 3E shows, the addition of H1 to the arrays did produce the expected protection of a DNA fragment larger than the core particle size DNA (the latter is protected by the core histones). Note that both the core and the chromatosome DNA fragments are seemingly longer on these gels than the expected 146 bp and 168 bp for the core and chromatosome DNA, respectively. This anomalous electrophoretic behavior of the *L. variegates* 208 bp sequence has been observed before (53, 58) and attributed to a slight curvature in the sequence.

Reconstituted chromatin fibers were imaged under the same conditions as fibers isolated from cells (Fig. 4). Fibers were again deposited on the surface from low ionic strength buffer, i.e., they were in their most extended state. In the case of control nucleosomal arrays [in the absence (Fig. 4A) or presence of LHs (Fig. 4C)] or arrays reconstituted on SssI methylase-methylated DNA (Fig. 4B), the individual nucleosomes can be seen as discrete entities, well separated from each other. The broadening effect of the AFM tip causes all objects to look larger in the x-y dimension

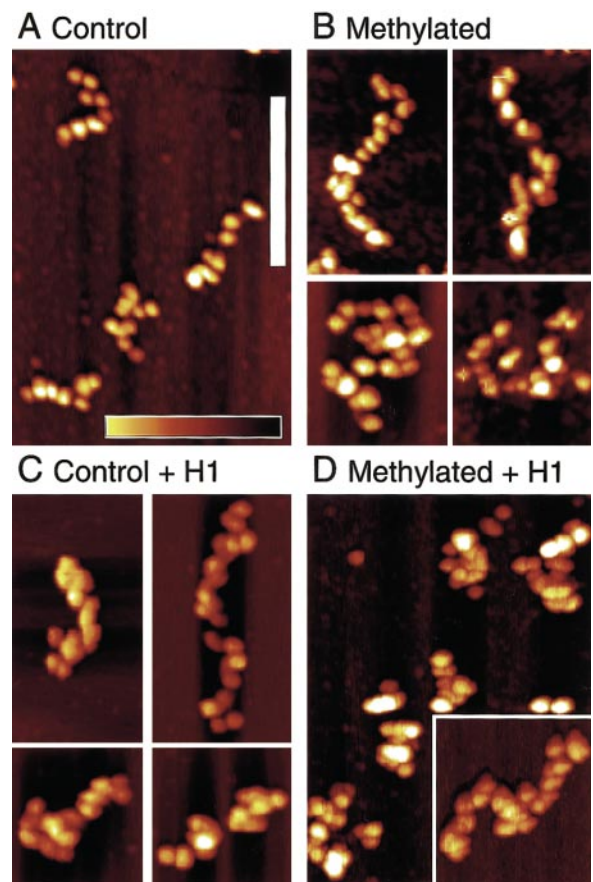


Figure 4. MacMode AFM images of chromatin fibers reconstituted on control and methylated 208–12 DNA sequence. Heights are 0–6 nm, as depicted in the horizontal bar. Vertical bar is 300 nm. *A*) Control nucleosomal arrays. *B*) Arrays reconstituted on methylated 208–12 DNA. *C*) Chromatin fibers after LH binding to control nucleosomal arrays. *D*) Chromatin fibers after LH binding to methylated arrays.

than they actually are, the extent of broadening depending on the dimensions of the apex of each individual tip. Thus, nucleosomes touching each other in images are actually spatially separated on the mica. The only morphological difference recognized by eye is in the case of reconstitutes on methylated DNA in the presence of LHs (Fig. 4D). In these fibers, the nucleosomes are much more crowded than in any of the three other cases, often with some particles partially hidden by others.

Internucleosomal center-to-center distances in reconstituted fibers

To gain quantitative characterization of the various reconstitutes, we measured center-to-center internucleosomal distances and constructed frequency distribution histograms (Fig. 5). In all cases, there was a bimodal distribution in this parameter, with two peaks centered ~ 25 nm and 33 nm (see double Gaussian fits); the only difference among the various chromatin preparations was in the relative proportion of the two peaks (see below).

One possible explanation for the appearance of the ~ 25 nm and ~ 33 nm peaks lies in the existence, in each 208 bp repeat, of two or more minor nucleosome positions near the major one (Fig. 3B) (53, 54). Determination of the location of the 146 bp fragment protected from MNase hydrolysis in nucleosomal arrays reconstituted on the 208–18 repeat showed that a large proportion of the nucleosome particles occupy a unique position on each repeat, with some less populated sites located around this major site (53, 54) (Fig. 3B).

From measurements in AFM images, our mean center-to-center distance was ~ 29 nm for Fig. 5A–C. In simple modeling, starting with a perfect fiber with an exact internucleosomal center-to-center spacing of 29 nm (Fig. 5E, a), a bimodal distribution became visible if $> 30\%$ of the nucleosomes occupy minor positioning sites ± 10 bp from the major site (Fig. 5E, b). A further increase in the number of nucleosomes occupying minor positions to $\sim 42\%$ (see legend to Fig. 5) may lead to an increase in the relative proportion of the ~ 25 nm peak (Fig. 5E, c). The number of nucleosomes occupying minor positions used in our modeling agrees generally with the experimental finding that only $\sim 50\%$ of the nucleosomes occupy the major position (53).

Thus, both the bimodal character of the center-to-center distance distribution curves and the peak height variations in these distributions (Fig. 5) may be explained by differences in the relative occupancy of the available nucleosome positions. Relative occupancies can be modeled by $N_i/N_o = \exp(-(E_i - E_o)/k_bT)$ where N_i and N_o are the occupancies of minor position i and major position o , respectively, E_i and E_o are the free energies of these positions, k_b is the Boltzmann constant, and T is the absolute temperature. Using a similar equation, Dong et al. (53) suggested a range of

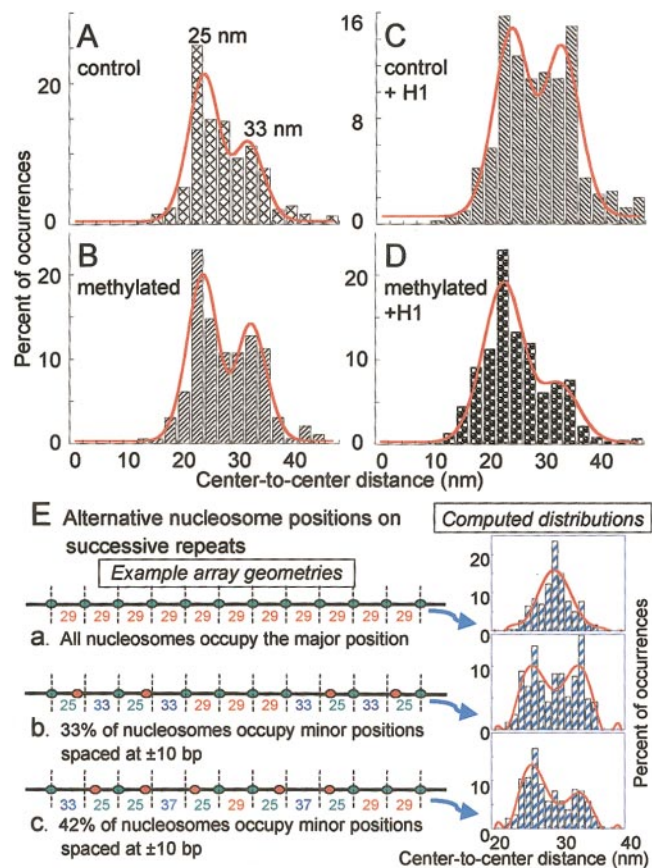


Figure 5. Normalized distributions of distances between centers of adjacent nucleosomes in reconstituted chromatin fibers: experiment (A–D) and modeling (E). A) Control nucleosomal arrays. B) Arrays reconstituted on methylated 208–12 DNA. C) Chromatin fibers after LH binding to control nucleosomal arrays. D) Chromatin fibers after LH binding to methylated arrays. Mean center-to-center distances \pm SE are 29 ± 1 nm (A–C) and 26 ± 1 nm (D). Note the bimodal distributions in all four cases and the changed ratio of the second to the first peak. Gaussian fits to the distributions are also presented. E) Nucleosomal array geometry and center-to-center distance distribution histograms as a function of alternative nucleosome positions on consecutive repeats (modeling). a) When most ($> 90\%$) of nucleosomes occupy the major position on all repeats (left), the center-to-center distance distribution will have one maximum at ~ 29 nm, as shown on the right. The spread in the distribution is due to randomization of the length of the linker DNA (± 5 bp) and nucleosomes ($< 10\%$) occupying minor sites. b) When 33% of the nucleosomes occupy minor positions (spaced at ± 10 bp) symmetrically (to either the right or left of the major position, in equal proportions), the frequency distribution becomes bimodal with peaks centered at 25 and 33 nm. c) When 42% of nucleosomes occupy minor positions in an asymmetric way, the frequency distribution will look like the respective histogram to the right. Note the change in the relative proportion of the two peaks (see text).

energy differences ($E_i - E_o$) on the order of 0.84 to 2.2 k_bT for the alternative nucleosome positions on this sequence. We used a somewhat narrower energy variation range of 0.7–1.3 k_bT because our modeling took into account only two minor positions (Dong et al. took into consideration four and more positions). We found

that such modeling of relative occupancies produces two peaks with the same two maxima in the center-to-center distance distribution as observed in the experiment (compare Fig. 5A, E).

If the two peaks in the distribution histograms of center-to-center internucleosomal distances are due to occupancy of alternative nucleosome positions on successive repeats, as suggested by our modeling, then the differences in the distributions for the different reconstitutes (Fig. 5) would be due to redistribution of the occupancy of these alternative positions. That LHs can affect the relative occupancy of alternative nucleosome particle positions (without creating new ones) has been convincingly reported for the same DNA construct (54). The relative proportions of the two peaks in the distribution histograms (Fig. 5C) suggest that LH binding causes more nucleosomes to occupy the major position than in the control nucleosomal array (the observed profile in the presence of LH resembles the modeled distribution in Fig. 5E, b, whereas that in the control array resembles the distribution in Fig. 5E, c). DNA methylation apparently does the same thing as H1, as judged by the increased second peak in Fig. 5B.

Once we are reasonably convinced that the relative magnitudes of the two peaks in the distribution histograms reflect redistribution of nucleosome positions, let us turn to the case where methylated DNA was reconstituted with both core histones and H1 (Fig. 5D). Since we observed an increase in the 33 nm peak in the two separate cases of methylated chromatin and control chromatin with H1, the combination of methylation and H1 was expected to lead to at least the same, if not a greater, increase in the area of this 33 nm peak. Instead, the opposite was observed. We hypothesize that this peculiar distribution reflects an independent event: compaction of the fiber.

Such a LH/DNA methylation-mediated compaction is corroborated by the significant increase in the number of nucleosomes per 10 nm of fiber contour length (Fig. 6A). The frequency distribution histograms show that the control (minus or plus H1) reconstitutes and, in the absence of H1, on methylated templates form a peak with a mean number of 0.48 ± 0.01 (the distributions were so close in the three separate cases that we present them as a combined distribution). In contrast, the distribution on the LH-containing methylated reconstitute centers $\sim 0.67 \pm 0.02$, indicating a compaction of a factor of ~ 1.4 compared with the other three cases.

Linker histone/DNA methylation-mediated compaction as seen by MNase digestion or sucrose density gradient sedimentation

To confirm the compaction seen in the AFM images, we used more conventional approaches. First, we compared the kinetics of MNase digestion on the different reconstitutes. As Fig. 6B demonstrates, the methylated reconstitute containing histone H1 was digested more

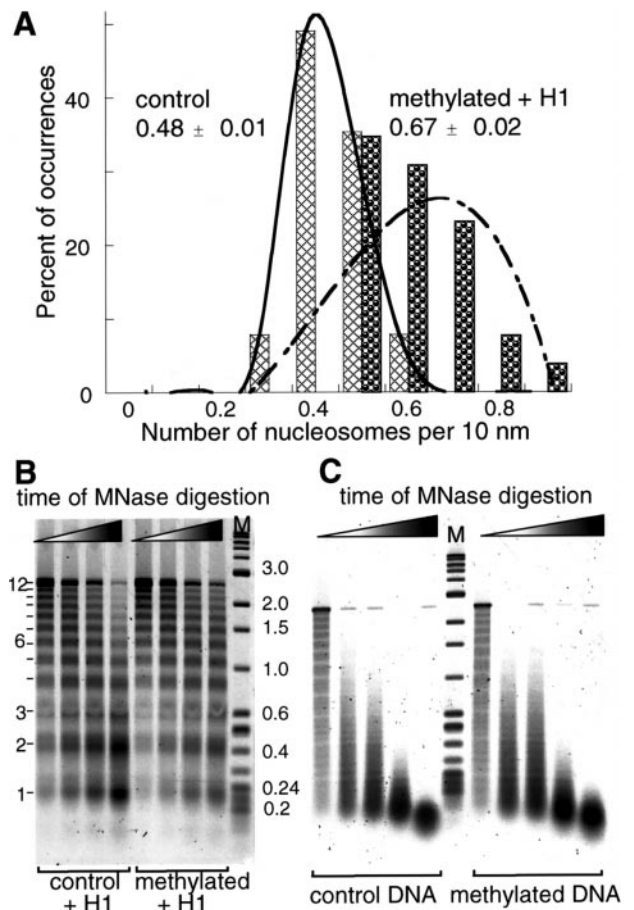


Figure 6. A) Number of nucleosomes per 10 nm of fiber contour length. Data for the control (in the absence or presence of LH) and methylated reconstitutes are presented as a common peak since they were indistinguishable. Mean numbers \pm SE are 0.48 ± 0.01 for the control and 0.67 ± 0.02 for the methylated+H1 reconstitute, respectively. Gaussian fits are overlaid to demonstrate the shift in that parameter. B) MNase digestion of control and methylated chromatin fibers, both reconstituted with H1. Digestion proceeded for 10, 20, 30, or 40 min (triangle) with $2 \text{ U}/\mu\text{l}$ of MNase at 37°C . Lanes M, size markers. Numbers on left side of gel indicate the nucleosomal ladder. C) MNase digestion of naked DNA controls.

slowly than the corresponding H1-containing control reconstitute. Quantitation of the rate of appearance of mononucleosome particles in the course of digestion (not shown) confirmed the visual impression from the gel patterns. Control digestion experiments performed on unmethylated or methylated naked DNA revealed no difference between the two DNA substrates (Fig. 6C). Since the only difference between the digested reconstitutes was the methylation status of the DNA, we concluded that the MNase digestion results corroborated the compaction seen in the AFM experiments and that the presence of H1 alone was not sufficient to drive the compaction. Similar comparisons between control and methylated reconstitutes that did not contain histone H1 (not shown) also corroborated the AFM-based observation that methylation alone was not sufficient to compact the fiber. Thus, DNA methylation

must work in conjunction with histone H1 binding to cause chromatin fiber compaction.

In a second approach, we looked for differences in the sedimentation behavior of control H1-containing fibers and H1-containing fibers reconstituted on methylated DNA, by using sucrose density gradient centrifugation. The control H1-containing fibers were reconstituted on Cy5-labeled 208–12 DNA, this fiber and the H1-containing methylated reconstitutes were mixed in equal amounts and sedimented in the same centrifuge tube. Gradient samples were analyzed by agarose gel electrophoresis, and the distribution of the total and control material was followed by fluorescence scanning of the gels (the total DNA stained with SYBR Gold produced blue fluorescence, whereas the Cy-5-labeled control DNA fluoresced in red). **Figure 7A** presents the distribution of both fluorescence labels throughout the gradient, with the third line (solid) presenting the difference between the two profiles, corresponding to the distribution of the methylated material in the gradient. As expected, the methylated H1-containing chromatin fibers sedimented faster than the control fibers, again indicating higher degree of compaction for the former fibers. Two repetitions of this experiment gave the same result.

Unmethylated and methylated DNA templates are equally loaded with histone octamers

The above results could easily be explained if there were a difference in the affinity of the histone octamers to these two kinds of DNA templates. The MPE ladders were indistinguishable from each other, with the same level of background material, suggesting there were no significant differences in the saturation levels of the two templates with octamers. The importance of this issue demanded more stringent analysis. We used two restriction endonuclease-based assays. In the first assay, all four types of reconstitutes were digested with *DraI*, an enzyme that cuts close to the dyad axis of the major nucleosome position (see Fig. 3B), and the resulting DNA fragments were analyzed on agarose gels (Fig. 7B). All four reconstitutes were digested to a similar degree, with the majority of the material remaining undigested due to the protection of the cleavage site by the histone octamer.

In the second assay, introduced by Hansen et al. (52) as a way to estimate the average number of nucleosomes on repetitive templates, the nucleosomal arrays were digested with *EcoRI*, which cuts in the linker DNA, and then run on polyacrylamide native gels. If every repeat contained a bound octamer (100% saturation), digestion would yield just a single monosome band. If templates were subsaturated, the repeats free of nucleosomes would yield naked DNA fragments of the length of the *EcoRI* fragment (195 bp; note that there are two *EcoRI* sites in the 208 repeat). The ratio of monosome particle DNA to free DNA serves as a measure of the degree of saturation. As clearly seen in Fig. 7C, lanes 1 and 2, the methylated and control templates were

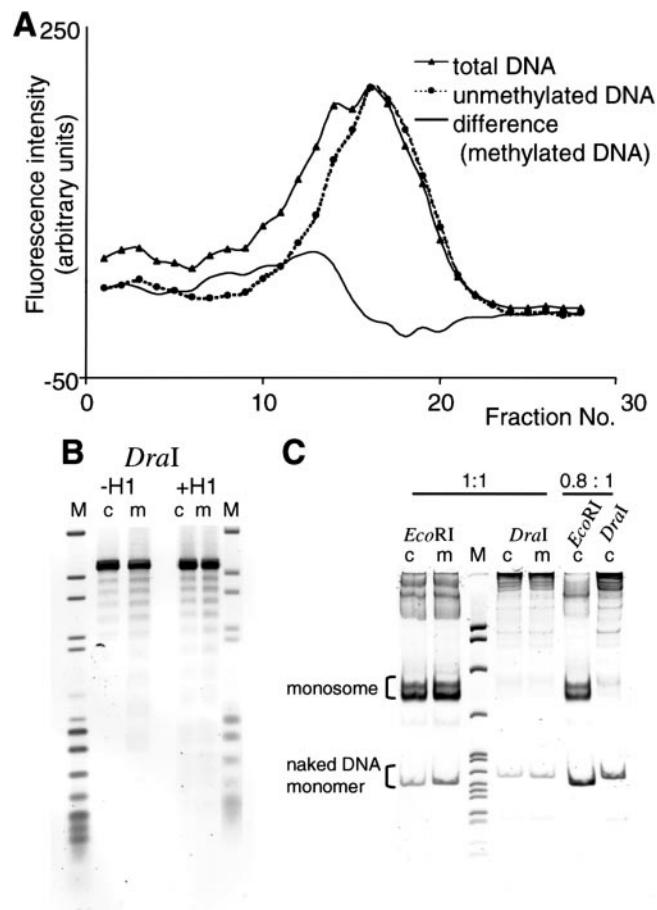


Figure 7. A) Sucrose density gradient centrifugation profile of control and methylated chromatin fibers, both reconstituted with H1. Gradient fractions were analyzed on 1% agarose gel. Gel was scanned and the intensity of fluorescence signals produced by SYBR Gold (total DNA) or Cy5 (control DNA) was estimated separately. The solid curve represents the difference (SYBR Gold minus Cy5) profile, corresponding to the methylated DNA. The reconstitute containing both methylated DNA and histone H1 is heavier (more compact) than the control reconstitute. B) *DraI* restriction patterns of control [c] and methylated [m] nucleosomal arrays in the absence or presence of H1 analyzed on 1.6% agarose gels. Lanes M, size markers. C) Restriction endonuclease assay of octamer loading on control [c] and methylated [m] nucleosomal arrays analyzed on 5.5% Duracryl gel. The restriction enzymes and the octamer/DNA weight ratios used are denoted above the lanes. Lane M, size markers.

equally saturated with octamers. The average number of nucleosomes per nucleosomal array was calculated to be 10.9 in the case of the control array and 10.5 for the methylated array, in general agreement with AFM observations. Digestion with *DraI*, although leaving the majority of the material undigested (see above), gave similar amounts of free DNA fragments for the control and the methylated template (compare lanes 4 and 5). Finally, lanes 6 and 7 demonstrate the sensitivity of the assay. Reducing the ratio of octamers to DNA from 1:1 in lanes 1, 2, 4, and 5, to 0.8:1 in lanes 6 and 7 led to a noticeable increase in the amount of free DNA (the average number of nucleosomes per control array dropped from 10.9 to 7.4).

Thus, it is clear that the LH/DNA methylation-mediated compaction observed is not due to different loading of the templates with nucleosomes. Nor apparently is it due to a difference in LH binding to both types of arrays, since the LH content was the same in both cases (results not shown), in agreement with published reports (17).

DISCUSSION

We have imaged, with the help of AFM, chromatin fibers isolated from control cultured fibroblasts and from fibroblasts treated with 3-ABA, an agent that causes hypermethylation of cellular DNA. Visual inspection of the AFM images, and quantitative assessment of center-to-center internucleosomal distances, angles between successive linkers, and number of nucleosomes per unit contour length of the fiber all show that the chromatin fibers isolated from 3-ABA-treated cells are more compact than their control counterparts even when deposited on the mica surface from low ionic strength buffer, i.e., in their most extended conformation. The fact that a difference between the two types of chromatin fibers can be detected even in their extended conformation suggests that the drug treatment alters some basic features of fiber structure; further investigation is needed to understand the molecular basis of such alteration.

We then used an *in vitro* reconstitution approach to dissect the molecular determinants of the DNA methylation-dependent chromatin compaction. The results based on examination of AFM images of different reconstitutes suggested that DNA methylation causes compaction of the chromatin fiber only in conjunction with the binding of LH to the fibers. Each condition alone, DNA methylation or LH binding, is necessary but not sufficient to compact chromatin fibers. The AFM conclusions were further substantiated by two independent biochemical approaches: MNase digestion and sucrose gradient density centrifugation.

It is gratifying that the degree of compaction observed (expressed as number of nucleosomes per 10 nm of contour fiber length) was very close *in vivo* and *in vitro*: ~ 0.46 for the control vs. ~ 0.70 for the hypermethylated chromatin fibers from the *in vivo* experiments and ~ 0.48 for the control vs. ~ 0.67 for the methylated H1-containing reconstituted fibers. Some discussion is warranted here. In the *in vivo* study we compared 'normal' fibers with hypermethylated ones; the *in vitro* experiments compare unmethylated substrates with highly methylated ones. If the effect of DNA methylation is dependent on its density along the DNA template, these seemingly different *in vivo* and *in vitro* templates may not be so different after all: the scattered methylatable CpGs in the genome may provide low methylation density, insufficient to affect the structure of bulk chromatin. On the other hand, the *in vivo* hypermethylated chromatin fiber may resemble, in its

methylation density, the methylated reconstitution substrate used in the *in vitro* experiments.

A second point concerns the role played by LHs in the DNA methylation-dependent chromatin compaction. We have demonstrated that LH binding is crucial for the compaction of methylated templates to occur. We must note that in the *in vivo* experiments there was no detectable difference in the amount of LHs present in the chromatin fibers isolated from control and treated cells, so that the *in vivo* compaction we observed may have involved LH binding. This statement may seem at odds with the results from an *in vivo* study on transcription from methylated templates microinjected in *Xenopus* oocytes (14). As pointed out by Bird and Wolffe (5), this methylation-dependent inhibition of transcription on chromatin templates occurred in the absence of the types of H1 normally associated with transcriptional repression. It is important, however, to bear in mind that other LH subtypes are present in the oocytes (59), and these may cooperate with DNA methylation to confer the compaction needed to repress transcription.

One last point concerns the lack of visible structural effect of histone H1 binding to control nucleosomal arrays (see Fig. 4C). We have demonstrated that histone H1 does bind properly to the fiber under the conditions used (e.g., Fig. 3E). The lack of visible effect on the fiber morphology may be because the reconstituted fibers are relatively short, only 12 nucleosomes in length. The reported zig-zag morphology of H1-containing fibers (39, 60) may remain undetectable in AFM images of such short fibers that may experience considerable distortion due to surface interactions and end effects. The lack of visible morphological effect of LH binding alone does not negate our main conclusion about the cooperation between LH binding and DNA methylation in producing chromatin fiber compaction, since it is based on positive evidence coming from both AFM and biochemical experiments.

In summary, our data indicate that the combined action of DNA methylation and LH binding is required to bring about chromatin compaction. This compaction may affect transcription of large chromatin domains. Compaction that affects specific gene transcription may require more complex interactions involving targeted binding of methyl-DNA binding proteins, histone deacetylation, and probably other mechanisms. [F]

We thank Dr. C. Whiteford for assistance with cell culture. This work is supported in part by the Italian Ministry of University and Scientific and Technological Research and by the Consiglio Nazionale delle Ricerche (P.C.). S.H.L. is a National Cancer Institute Scholar.

REFERENCES

1. Costello, J. F., and Plass, C. (2001) Methylation matters. *J. Med. Genet.* **38**, 285-303
2. Razin, A., and Shemer, R. (1999) Epigenetic control of gene expression. *Results Prob. Cell Differ.* **25**, 189-204

3. Feil, R., and Khosla, S. (1999) Genomic imprinting in mammals: an interplay between chromatin and DNA methylation? *Trends Genet.* **15**, 431–435
4. Tilghman, S. M. (1999) The sins of the fathers and mothers: genomic imprinting in mammalian development. *Cell* **96**, 185–193
5. Bird, A. P., and Wolffe, A. P. (1999) Methylation-induced repression—belts, braces, and chromatin. *Cell* **99**, 451–454
6. Hendrich, B. (2000) Methylation moves into medicine. *Curr. Biol.* **10**, R60–R63
7. Robertson, K. D., and Jones, P. A. (2000) DNA methylation: past, present and future directions. *Carcinogenesis* **21**, 461–467
8. Meehan, R. R., Lewis, J. D., McKay, S., Kleiner, E. L., and Bird, A. P. (1989) Identification of a mammalian protein that binds specifically to DNA containing methylated CpGs. *Cell* **58**, 499–507
9. Nan, X., Campoy, F. J., and Bird, A. (1997) MeCP2 is a transcriptional repressor with abundant binding sites in genomic chromatin. *Cell* **88**, 471–481
10. Hendrich, B., and Bird, A. (1998) Identification and characterization of a family of mammalian methyl-CpG binding proteins. *Mol. Cell. Biol.* **18**, 6538–6547
11. Razin, A. (1998) CpG methylation, chromatin structure and gene silencing—a three-way connection. *EMBO J.* **17**, 4905–4908
12. Ng, H. H., and Bird, A. (1999) DNA methylation and chromatin modification. *Curr. Opin. Genet. Dev.* **9**, 158–163
13. Buschhausen, G., Wittig, B., Graessmann, M., and Graessmann, A. (1987) Chromatin structure is required to block transcription of the methylated herpes simplex virus thymidine kinase gene. *Proc. Natl. Acad. Sci. USA* **84**, 1177–1181
14. Kass, S. U., Landsberger, N., and Wolffe, A. P. (1997) DNA methylation directs a time-dependent repression of transcription initiation. *Curr. Biol.* **7**, 157–165
15. Kass, S. U., Goddard, J. P., and Adams, R. L. (1993) Inactive chromatin spreads from a focus of methylation. *Mol. Cell. Biol.* **13**, 7372–7379
16. Felsenfeld, G., Nickol, J., Behe, M., McGhee, J., and Jackson, D. (1983) Methylation and chromatin structure. *Cold Spring Harbor Symp. Quant. Biol.* **47**, 577–584
17. Nightingale, K., and Wolffe, A. P. (1995) Methylation at CpG sequences does not influence histone H1 binding to a nucleosome including a *Xenopus borealis* 5 S rRNA gene. *J. Biol. Chem.* **270**, 4197–4200
18. Drew, H. R., and McCall, M. J. (1987) Structural analysis of a reconstituted DNA containing three histone octamers and histone H5. *J. Mol. Biol.* **197**, 485–511
19. Englander, E. W., Wolffe, A. P., and Howard, B. H. (1993) Nucleosome interactions with a human Alu element. Transcriptional repression and effects of template methylation. *J. Biol. Chem.* **268**, 19565–19573
20. Davey, C., Pennings, S., and Allan, J. (1997) CpG methylation remodels chromatin structure in vitro. *J. Mol. Biol.* **267**, 276–288
21. Keshet, I., Lieman-Hurwitz, J., and Cedar, H. (1986) DNA methylation affects the formation of active chromatin. *Cell* **44**, 535–543
22. Caiafa, P., Attina, M., Cacace, F., Tomassetti, A., and Strom, R. (1986) 5-Methylcytosine levels in nucleosome subpopulations differently involved in gene expression. *Biochim. Biophys. Acta* **867**, 195–200
23. Zardo, G., D'Erme, M., Reale, A., Strom, R., Perilli, M., and Caiafa, P. (1997) Does poly(ADP-ribosyl)ation regulate the DNA methylation pattern? *Biochemistry* **36**, 7937–7943
24. Zardo, G., and Caiafa, P. (1998) The unmethylated state of CpG islands in mouse fibroblasts depends on the poly(ADP-ribosyl)ation process. *J. Biol. Chem.* **273**, 16517–16520
25. de Capoa, A., Febbo, F. R., Giovannelli, F., Niveleau, A., Zardo, G., Marenzi, S., and Caiafa, P. (1999) Reduced levels of poly(ADP-ribosyl)ation result in chromatin compaction and hypermethylation as shown by cell-by-cell computer-assisted quantitative analysis. *FASEB J.* **13**, 89–93
26. Zardo, G., Marenzi, S., Perilli, M., and Caiafa, P. (1999) Inhibition of poly(ADP-ribosyl)ation introduces an anomalous methylation pattern in transfected foreign DNA. *FASEB J.* **13**, 1518–1522
27. Yager, T. D., McMurray, C. T., and van Holde, K. E. (1989) Salt-induced release of DNA from nucleosome core particles. *Biochemistry* **28**, 2271–2281
28. Leuba, S. H., Zlatanova, J., and van Holde, K. (1994) On the location of linker DNA in the chromatin fiber. Studies with immobilized and soluble micrococcal nuclease. *J. Mol. Biol.* **235**, 871–880
29. Laemmli, U. K. (1970) Cleavage of structural proteins during the assembly of the head of bacteriophage T4. *Nature (London)* **227**, 680–685
30. Georgel, P., Demeler, B., Terpening, C., Paule, M. R., and van Holde, K. E. (1993) Binding of the RNA polymerase I transcription complex to its promoter can modify positioning of downstream nucleosomes assembled in vitro. *J. Biol. Chem.* **268**, 1947–1954
31. von Holt, C., Brandt, W. F., Greyling, H. J., Lindsey, G. G., Retief, J. D., Rodrigues, J. D., Schwager, S., and Sewell, B. T. (1989) Isolation and characterization of histones. *Methods Enzymol.* **170**, 431–523
32. Leuba, S. H., Bustamante, C., van Holde, K., and Zlatanova, J. (1998) Linker histone tails and N-tails of histone H3 are redundant: scanning force microscopy studies of reconstituted fibers. *Biophys. J.* **74**, 2830–2839
33. Tatchell, K., and van Holde, K. E. (1977) Reconstitution of chromatin core particles. *Biochemistry* **16**, 5295–5303
34. Hertzberg, R. P., and Dervan, P. B. (1984) Cleavage of DNA with methidiumpropyl-EDTA-iron(II): reaction conditions and product analyses. *Biochemistry* **23**, 3934–3945
35. Cartwright, I. L., and Elgin, S. C. (1989) Nonenzymatic cleavage of chromatin. *Methods Enzymol.* **170**, 359–369
36. Zlatanova, J., Leuba, S. H., Yang, G., Bustamante, C., and van Holde, K. (1994) Linker DNA accessibility in chromatin fibers of different conformations: a reevaluation. *Proc. Natl. Acad. Sci. USA* **91**, 5277–5280
37. Leuba, S. H., Yang, G., Robert, C., Samori, B., van Holde, K., Zlatanova, J., and Bustamante, C. (1994) Three-dimensional structure of extended chromatin fibers as revealed by tapping-mode scanning force microscopy. *Proc. Natl. Acad. Sci. USA* **91**, 11621–11625
38. Leuba, S. H., and Bustamante, C. (1999) Analysis of chromatin by scanning force microscopy. *Methods Mol. Biol.* **119**, 143–160
39. Leuba, S. H., Bustamante, C., Zlatanova, J., and van Holde, K. (1998) Contributions of linker histones and histone H3 to chromatin structure: scanning force microscopy studies on trypsinized fibers. *Biophys. J.* **74**, 2823–2829
40. Rankin, P. W., Jacobson, E. L., Benjamin, R. C., Moss, J., and Jacobson, M. K. (1989) Quantitative studies of inhibitors of ADP-ribosylation in vitro and in vivo. *J. Biol. Chem.* **264**, 4312–4317
41. Zardo, G., Marenzi, S., and Caiafa, P. (1998) H1 histone as a trans-acting factor involved in protecting genomic DNA from full methylation. *Biol. Chem.* **379**, 647–654
42. Poirier, G. G., de Murcia, G., Jongstra-Bilen, J., Niedergang, C., and Mandel, P. (1982) Poly(ADP-ribosyl)ation of polynucleosomes causes relaxation of chromatin structure. *Proc. Natl. Acad. Sci. USA* **79**, 3423–3427
43. Lewis, J., and Bird, A. (1991) DNA methylation and chromatin structure. *FEBS Lett.* **285**, 155–159
44. Zlatanova, J., Leuba, S. H., and van Holde, K. (1998) Chromatin fiber structure: morphology, molecular determinants, structural transitions. *Biophys. J.* **74**, 2554–2566
45. van Holde, K. E. (1988) *Chromatin*, Springer-Verlag, New York
46. Gunjan, A., Alexander, B. T., Sittman, D. B., and Brown, D. T. (1999) Effects of H1 histone variant overexpression on chromatin structure. *J. Biol. Chem.* **274**, 37950–37956
47. van Holde, K., and Zlatanova, J. (1996) What determines the folding of the chromatin fiber? *Proc. Natl. Acad. Sci. USA* **93**, 10548–10555
48. Zlatanova, J., Leuba, S. H., and van Holde, K. (1999) Chromatin structure revisited. *Crit. Rev. Eukaryot. Gene Exp.* **9**, 245–255
49. Bednar, J., Horowitz, R. A., Grigoryev, S. A., Carruthers, L. M., Hansen, J. C., Koster, A. J., and Woodcock, C. L. (1998) Nucleosomes, linker DNA, and linker histone form a unique structural motif that directs the higher-order folding and compaction of chromatin. *Proc. Natl. Acad. Sci. USA* **95**, 14173–14178
50. Huletsky, A., de Murcia, G., Muller, S., Hengartner, M., Menard, L., Lamarre, D., and Poirier, G. G. (1989) The effect of poly(ADP-ribosyl)ation on native and H1-depleted chromatin. A

- role of poly(ADP-ribosyl)ation on core nucleosome structure. *J. Biol. Chem.* **264**, 8878–8886
51. Simpson, R. T., Thoma, F., and Brubaker, J. M. (1985) Chromatin reconstituted from tandemly repeated cloned DNA fragments and core histones: a model system for study of higher order structure. *Cell* **42**, 799–808
 52. Hansen, J. C., Ausio, J., Stanik, V. H., and van Holde, K. E. (1989) Homogeneous reconstituted oligonucleosomes, evidence for salt-dependent folding in the absence of histone H1. *Biochemistry* **28**, 9129–9136
 53. Dong, F., Hansen, J. C., and van Holde, K. E. (1990) DNA and protein determinants of nucleosome positioning on sea urchin 5S rRNA gene sequences in vitro. *Proc. Natl. Acad. Sci. USA* **87**, 5724–5728
 54. Meersseman, G., Pennings, S., and Bradbury, E. M. (1991) Chromatosome positioning on assembled long chromatin. Linker histones affect nucleosome placement on 5 S rDNA. *J. Mol. Biol.* **220**, 89–100
 55. Pennings, S., Meersseman, G., and Bradbury, E. M. (1991) Mobility of positioned nucleosomes on 5 S rDNA. *J. Mol. Biol.* **220**, 101–110
 56. Antequera, F., and Bird, A. (1999) CpG islands as genomic footprints of promoters that are associated with replication origins. *Curr. Biol.* **9**, R661–667
 57. Simpson, R. T. (1978) Structure of the chromatosome, a chromatin particle containing 160 base pairs of DNA and all the histones. *Biochemistry* **17**, 5524–5531
 58. An, W., Leuba, S. H., van Holde, K., and Zlatanova, J. (1998) Linker histone protects linker DNA on only one side of the core particle and in a sequence-dependent manner. *Proc. Natl. Acad. Sci. USA* **95**, 3396–3401
 59. Khochbin, S., and Wolffe, A. P. (1994) Developmentally regulated expression of linker histone variants in vertebrates. *Eur. J. Biochem.* **225**, 501–510
 60. Thoma, F., Koller, T., and Klug, A. (1979) Involvement of histone H1 in the organization of the nucleosome and of the salt-dependent superstructures of chromatin. *J. Cell Biol.* **83**, 403–427

*Received for publication May 2, 2001.
Revised for publication August 27, 2001.*